J. Phys. B: At. Mol. Opt. Phys. **33** (2000) 343–352. Printed in the UK PII: S0953-4075(00)06689-X

Solving quantum eigenvalue problems by discrete singular convolution

G W Wei

Department of Computational Science, National University of Singapore, Singapore 117543, Singapore

Received 4 August 1999, in final form 19 October 1999

Abstract. This paper explores the utility of a discrete singular convolution (DSC) algorithm for solving the Schrödinger equation. DSC kernels of Shannon, Dirichlet, modified Dirichlet and de la Vallée Poussin are selected to illustrate the present algorithm for obtaining eigenfunctions and eigenvalues. Four benchmark physical problems are employed to test numerical accuracy and speed of convergence of the present approach. Numerical results indicate that the present approach is efficient and reliable for solving the Schrödinger equation.

1. Introduction

There is an ongoing interest in computational methodology [1–20]. Most efforts are centred on developing either global or local methods for solving a variety of time-dependent and time-independent problems. The well known local methods involve finite differences, finite elements, finite volumes and boundary elements. Local methods are flexible for handling complex boundary and geometry, but are not as accurate as global methods. Global approximations to a function and its derivatives are typically realized by a set of truncated basis expansions which result in a finite approximation. Global methods are highly localized at their spectral representations and thus they provide high computational accuracy. However, they are not convenient for complex boundary and geometry such as occur in waveguide problems. It is desirable to have methods which combine global methods' accuracy with local methods' flexibility for practical applications.

Discrete singular convolution (DSC) [21] was proposed as a potential numerical approach for solving many computational problems, including linear and nonlinear dynamics [22], Hilbert transform, processing of analytic signals, and computational tomography. Based on the DSC formalism, a unification was achieved [23] for computational methods of the global, local, finite difference, finite element, finite volume, Galerkin, collocation, subdomain and Ritz variational types. The underlying mathematical structure of the DSC approach is the theory of distributions. Heaviside and Dirac had exploited the use of the delta distribution before Sobolev, Schwartz [24], Korevaar [25] and others put the distribution theory into a rigorous mathematical form. More general orthogonal series analyses of the delta distribution were studied by Walter [27] and others [28–30]. The numerical use of many delta sequences as probability density estimators was discussed by Walter and Blum [30] and others [29, 32, 33].

The purpose of this paper is to explore the utility of the DSC algorithm for the numerical solution of the Schrödinger equation. This is illustrated by numerically resolving eigenfunctions and eigenvalues. This paper is organized as follows. Section 2 gives a brief

0953-4075/00/030343+10$30.00

review of the DSC formalism. The reader is referred to the original work [21] for more details. Numerical eigenvalue results are presented in section 3. Four important problems, an I_2 Morse potential, a two-dimensional (2D) harmonic oscillator, a three-dimensional (3D) harmonic oscillator, and a non-polynomial oscillator (NPO) are selected for illustration. The paper ends with a conclusion.

2. Discrete singular convolution

Singular convolutions appear in many problems, such as Hilbert transform, Abel transform and Radon transforms. DSC is a general approach for numerically solving singular convolution problems. By appropriate realizations of a singular convolution kernel, the DSC can be an extremely efficient, accurate and reliable algorithm for scientific computations.

Let T be a distribution and $\eta(t)$ be an element of the space of test functions. A singular convolution can be defined as

$$F(t) = (T * \eta)(t) = \int_{-\infty}^{\infty} T(t-x)\eta(x)\,\mathrm{d}x. \tag{1}$$

Here $T(t-x)$ is a singular kernel. An interesting example is the singular kernels of the *delta type*

$$T(x) = \delta^{(n)}(x), \qquad (n = 0, 1, 2, \ldots), \tag{2}$$

where kernel $T(x) = \delta(x)$ is important for interpolation of surfaces and curves (including atomic, molecular and biological potential energy surfaces) and $T(x) = \delta^{(n)}(x)$ $(n = 1, 2, \ldots)$ are essential for numerically solving partial differential equations. However, since these kernels are singular, they cannot be directly digitized in computers. Hence, the singular convolution, equation (1), is of little numerical merit. To avoid the difficulty of using singular expressions directly in computers, sequences of approximations (T_α) of the distribution T can be constructed

$$\lim_{\alpha \to \alpha_0} T_\alpha(x) \longrightarrow T(x), \tag{3}$$

where α_0 is a generalized limit. Obviously, in the case of $T(x) = \delta(x)$, the sequence, $T_\alpha(x)$, is a delta sequence. Furthermore, with a sufficiently smooth approximation, it makes sense to consider a DSC

$$F_\alpha(t) = \sum_k T_\alpha(t - x_k) f(x_k), \tag{4}$$

where $F_\alpha(t)$ is an approximation to $F(t)$ and $\{x_k\}$ is an appropriate set of discrete points on which the DSC (4) is well defined. Note that the original test function $\eta(x)$ has been replaced by $f(x)$. The mathematical property or requirement of $f(x)$ is determined by an approximate kernel T_α.

Shannon's kernel

$$\frac{\sin \alpha(x - x')}{\pi(x - x')}$$

is a special example for the delta sequence. Other important examples include the Dirichlet kernel

$$\frac{\sin[(l + \frac{1}{2})(x - x')]}{2\pi \sin[\frac{1}{2}(x - x')]},$$

the modified Dirichlet (MD) kernel

$$\frac{\sin[(l+\frac{1}{2})(x-x')]}{2\pi\tan[\frac{1}{2}(x-x')]},$$

and the de la Vallée Poussin (DLVP) kernel

$$\frac{1}{\pi\alpha}\frac{\cos[\alpha(x-x')]-\cos[2\alpha(x-x')]}{(x-x')^2}.$$

For sequences of delta type, an interpolating (or quasi-interpolating) algorithm sampling at *Nyquist frequency* ($\alpha=\frac{\pi}{\Delta}$) has advantage over a non-interpolating discretization

$$\frac{\sin[\alpha(x-x')]}{\pi(x-x')}\to\frac{\sin\frac{\pi}{\Delta}(x-x_k)}{\frac{\pi}{\Delta}(x-x_k)}. \tag{5}$$

The uniform, Nyquist rate, interpolating discretization is also used for the Dirichlet kernel:

$$\frac{\sin[(l+\frac{1}{2})(x-x')]}{2\pi\sin[\frac{1}{2}(x-x')]}\to\frac{\sin(\frac{\pi}{\Delta}(x-x_k))}{(2M+1)\sin(\frac{\pi}{\Delta}\frac{x-x_k}{2M+1})}. \tag{6}$$

In comparison with Shannon's kernel, the Dirichlet kernel has one more parameter M which can be optimized to achieve better results in computations. Usually, we set a sufficiently large M for various numerical applications. Obviously, the Dirichlet kernel converts to Shannon's kernel at the limit of $M\to\infty$. This uniform interpolating discretization will also be used for discretizing the MD kernel

$$\frac{\sin[(l+\frac{1}{2})(x-x')]}{2\pi\tan[\frac{1}{2}(x-x')]}\to\frac{\sin(\frac{\pi}{\Delta}(x-x_k))}{(2M+1)\tan(\frac{\pi}{\Delta}\frac{x-x_k}{2M+1})}, \tag{7}$$

and for the de la Vallée Poussin kernel

$$\frac{1}{\pi\alpha}\frac{\cos[\alpha(x-x')]-\cos[2\alpha(x-x')]}{(x-x')^2}\to\frac{2}{3}\frac{\cos\frac{\pi}{\Delta}(x-x_k)-\cos\frac{2\pi}{\Delta}(x-x_k)}{[\frac{\pi}{\Delta}(x-x_k)]^2}, \tag{8}$$

where $\bar{\Delta}=\frac{3}{2}\Delta$. Since π/Δ is proportional to the highest frequency which can be reached in the Fourier representation, the Δ should be very small for a given problem involving very oscillatory functions or very high frequency components.

In the DSC approach we choose a grid representation for the coordinate so that the potential part, $V(x)$, of the Hamiltonian is diagonal. The full DSC matrix representation for the Hamiltonian operator, H, is given by

$$H(x_j,x_k)=-\frac{\hbar^2}{2m}\delta_\alpha^{(2)}(x_j-x_k)+V(x_j)\delta_{j,k}, \tag{9}$$

where m is the mass of the Hamiltonian system and $\delta_\alpha^{(2)}(x_j-x_k)$ is *analytically* given by

$$\delta_\alpha^{(2)}(x_j-x_k)=\left[\left(\frac{\mathrm{d}}{\mathrm{d}x}\right)^2\delta_\alpha(x-x_k)\right]_{x=x_j}. \tag{10}$$

Here $\delta_\alpha(x-x_k)$ is a collective symbol for any of the right-hand sides of equations (5)–(8). Extending to higher dimensions is obvious. Equation (9) or its multidimensional extension is referred to as a DSC-Hamiltonian matrix.

3. Results

In this paper, we limit our attention to DSC kernels of the Shannon, DLVP, Dirichlet and MD type. Nevertheless, various other DSC kernels can be similarly employed. Note that DSC kernels of Shannon and DLVP are parameter free, which is convenient for applications. The $2M+1$ parameter used for other two kernels is chosen as 71 for all calculations. We note that as long as the $2M+1$ value is chosen sufficiently large ($2M+1 > W$, where $2W+1$ is the matrix bandwidth), the numerical results are not sensitive to specific values used. When a potential is given, eigenvalues are obtained by a direct diagonalization of the DSC-Hamiltonian matrix, equation (9) or its multidimensional generalization.

To illustrate the use of the DSC algorithm and test its accuracy for calculating eigenfunctions and eigenvalues, we consider four benchmark problems: the Morse potential for an I_2 molecule, a 2D harmonic oscillator, a 3D harmonic oscillator and an NPO. A general form for the Schrödinger equation in the coordinate representation is given by

$$\left[-\frac{\hbar^2}{2m} \sum_{i=1}^{n} \frac{\partial^2}{\partial x_i^2} + V(x_1, \ldots, x_n) \right] \Phi_k(x_1, \ldots, x_n) = E_k \Phi_k(x_1, \ldots, x_n), \tag{11}$$

where Φ_k and E_k are the kth eigenfunction and eigenvalue respectively.

3.1. The I_2 molecule

The Morse potential for the I_2 molecule is given by

$$V(x) = D[e^{-2\alpha x} - 2e^{-\alpha x} + 1], \tag{12}$$

where $D = 0.0224$ and $\alpha = 0.9374$. Here, the reduced mass for the Schrödinger equation is $m = 119\,406$. The anharmonic character of the Morse potential allows dissociation, hence it is one of the most popular potentials for modelling the spectroscopy and dynamics of the I_2 molecule. The Schrödinger equation of the I_2 Morse system is actually solvable. Exact eigenfunctions are well known generalized Laguerre polynomials [34]

$$\Phi_k = N_k z^{\frac{p}{2}} e^{-\frac{z}{2}} L_k^p(z), \tag{13}$$

where $z = \beta e^{-\alpha x}$, $p = \beta - 2k - 1$ and $\beta = 156.047\,612\,535$. Here, N_k is a normalization constant and is given by [34]

$$N_k = \left[\frac{\Gamma(p)}{\alpha} \sum_{\gamma=0}^{k} (-1)^\gamma \binom{-p}{\gamma} \right]^{-1/2}. \tag{14}$$

Exact eigenvalues of the I_2 molecule are [34]

$$E_k = \kappa \left[k + \frac{1}{2} - \frac{1}{\beta} \left(k + \frac{1}{2} \right)^2 \right], \tag{15}$$

where $\kappa = 5.741\,837\,286 \times 10^{-4}$ is calculated according to the physical property of I_2. Since κ is very small, the density of state of this system is obviously very high. Thus it often serves as a standard problem for testing new numerical algorithms.

In a recent study, Braun *et al* [18] have used this system to test their efficient Chebyshev–Lanczos method. They achieve a remarkably high accuracy which ranges from 7 to 9 digits using 128 grid points. For DSC kernels of Shannon, Dirichlet and MD, we choose 64 grid points ($N = 64$) which corresponds to the grid spacing of 0.043 077 ($\Delta = 0.043\,077$). All grid points x_k are equally distributed in the interval $[-\frac{\Delta(N+1)}{2}, \frac{\Delta(N+1)}{2}]$. For a comparison, we list our calculation and those of Braun *et al* [18] in table 1. Our 64 grid point results are 200

Table 1. Comparison of errors for I_2 Morse oscillator.

k	Analytical	Braun *et al* ($N = 128$)	Shannon ($N = 64$)	Dirichlet ($N = 64$)	MD ($N = 64$)	DLVP ($N = 96$)
0	0.852 996 623 626 6942(−03)	−0.10(−10)	−0.14(−13)	−0.14(−13)	−0.14(−13)	−0.14(−13)
1	0.141 246 218 462 9706(−02)	−0.30(−10)	−0.42(−13)	−0.42(−13)	−0.42(−13)	−0.42(−13)
2	0.196 456 866 183 4224(−02)	−0.50(−10)	−0.70(−13)	−0.70(−13)	−0.70(−13)	−0.70(−13)
3	0.250 931 605 524 0247(−02)	−0.70(−10)	−0.97(−13)	−0.97(−13)	−0.97(−13)	−0.97(−13)
4	0.304 670 436 484 7777(−02)	−0.89(−10)	−0.12(−12)	−0.12(−12)	−0.12(−12)	−0.12(−12)
5	0.357 673 359 065 6813(−02)	−0.11(−09)	−0.15(−12)	−0.15(−12)	−0.15(−12)	−0.15(−12)
6	0.409 940 373 266 7354(−02)	−0.13(−09)	−0.18(−12)	−0.18(−12)	−0.18(−12)	−0.18(−12)
7	0.461 471 479 087 9402(−02)	−0.15(−09)	−0.20(−12)	−0.20(−12)	−0.20(−12)	−0.20(−12)
8	0.512 266 676 529 2955(−02)	−0.16(−09)	−0.23(−12)	−0.23(−12)	−0.23(−12)	−0.23(−12)
9	0.562 325 965 590 8014(−02)	−0.18(−09)	−0.25(−12)	−0.28(−12)	−0.25(−12)	−0.25(−12)
10	0.611 649 346 272 4579(−02)	−0.20(−09)	−0.28(−12)	−0.28(−12)	−0.28(−12)	−0.28(−12)
11	0.660 236 818 574 2650(−02)	−0.22(−09)	−0.30(−12)	−0.30(−12)	−0.30(−12)	−0.30(−12)
12	0.708 088 382 496 2227(−02)	−0.23(−09)	−0.33(−12)	−0.33(−12)	−0.33(−12)	−0.33(−12)
13	0.755 204 038 038 3310(−02)	−0.25(−09)	−0.35(−12)	−0.35(−12)	−0.35(−12)	−0.35(−12)
14	0.801 583 785 200 5899(−02)	−0.27(−09)	−0.37(−12)	−0.37(−12)	−0.37(−12)	−0.37(−12)
15	0.847 227 623 982 9993(−02)	−0.28(−09)	−0.39(−12)	−0.39(−12)	−0.39(−12)	−0.40(−12)
16	0.892 135 554 385 5595(−02)	−0.30(−09)	−0.41(−12)	−0.41(−12)	−0.41(−12)	−0.41(−12)
17	0.936 307 576 408 2702(−02)	−0.32(−09)	−0.42(−12)	−0.42(−12)	−0.42(−12)	−0.43(−12)
18	0.979 743 690 051 1314(−02)	−0.33(−09)	−0.42(−12)	−0.42(−12)	−0.42(−12)	−0.43(−12)
19	0.102 244 389 531 4143(−01)	−0.35(−09)	−0.39(−12)	−0.39(−12)	−0.39(−12)	−0.39(−12)
20	0.106 440 819 219 7306(−01)	−0.36(−09)	−0.29(−12)	−0.30(−12)	−0.29(−12)	−0.28(−12)
21	0.110 563 658 070 0619(−01)	−0.38(−09)	0.13(−12)	0.13(−12)	0.13(−12)	−0.10(−13)
22	0.114 612 906 082 4082(−01)	−0.39(−09)	0.14(−11)	0.14(−11)	0.14(−11)	0.61(−12)
23	0.118 588 563 256 7697(−01)	−0.41(−09)	0.29(−11)	0.29(−11)	0.29(−11)	0.19(−11)
24	0.122 490 629 593 1461(−01)	−0.42(−09)	0.17(−11)	0.17(−11)	0.18(−11)	0.46(−11)

to 1000 times more accurate than those of Braun *et al*, obtained by using 128 grid points. It requires about 1.5 times as many grid points ($N = 96$) for the DLVP delta sequence kernel to achieve the same level of accuracy as those obtained by using other kernels.

3.2. A 2D harmonic oscillator

To illustrate further the accuracy and robustness of the DSC algorithm, we consider the 2D Schrödinger equation with a harmonic oscillator potential

$$V(x, y) = \tfrac{1}{2}(x^2 + y^2). \tag{16}$$

One of most important reasons for this choice is the analytical solvability of the model. By setting $\hbar = m = 1$ in the Schrödinger equation, analytical eigenvalues are given by

$$E_{n_x,n_y} = 1 + n_x + n_y = 1 + n, \tag{17}$$

with the degree of degeneracy of $d_n = n + 1$ in the nth energy level.

For DSC kernels of Shannon, Dirichlet and MD, the number of grid points used in each dimension is 26 ($N_x = N_y = 26$, $\Delta_x = \Delta_y = 0.481\,4815$). As listed in table 1, the first 21 eigenvalues are all accurate to at least ten significant figures. This calculation demonstrates that the DSC algorithm is extremely accurate for handling degenerate eigenvalue problems. Calculations obtained by using the DLVP delta sequence kernel are slightly less accurate. It requires 39 grid points in each dimension to reach the same accuracy as those obtained by using other kernels (26 grid points in each dimension). These results have also been presented in table 2 for a comparison of different kernels.

Table 2. Errors for the eigenvalues of the 2D harmonic oscillator.

n	d_n	Exact	Shannon ($N_x = N_y = 26$)	Dirichlet ($N_x = N_y = 26$)	MD ($N_x = N_y = 26$)	DLVP ($N_x = N_y = 39$)
0	1	1	0.71(−14)	0.30(−12)	0.24(−12)	0.92(−12)
1	2	2	0.25(−12)	0.21(−12)	0.27(−12)	0.64(−12)
			0.21(−12)	0.64(−13)	0.29(−12)	0.38(−12)
2	3	3	0.33(−12)	0.37(−12)	0.31(−12)	0.57(−12)
			0.26(−12)	0.23(−12)	0.50(−13)	0.19(−12)
			0.51(−13)	−0.89(−15)	−0.14(−12)	−0.41(−12)
3	4	4	0.18(−12)	0.36(−12)	0.38(−12)	0.15(−11)
			0.70(−13)	0.20(−12)	0.34(−13)	0.36(−12)
			0.19(−12)	−0.17(−12)	0.10(−12)	0.10(−12)
			−0.25(−12)	−0.25(−12)	−0.27(−13)	−0.31(−12)
4	5	5	0.46(−13)	0.31(−12)	0.33(−12)	0.13(−11)
			−0.22(−12)	−0.27(−12)	−0.40(−12)	0.51(−12)
			−0.40(−12)	−0.37(−12)	−0.40(−12)	0.20(−13)
			−0.14(−10)	−0.14(−10)	−0.14(−10)	−0.76(−11)
			−0.14(−10)	−0.14(−10)	−0.14(−10)	−0.85(−11)
5	6	6	−0.17(−12)	0.13(−12)	−0.90(−13)	0.58(−13)
			−0.33(−12)	−0.19(−12)	−0.22(−12)	−0.14(−12)
			−0.14(−10)	−0.14(−10)	−0.14(−10)	−0.76(−11)
			−0.14(−10)	−0.14(−10)	−0.14(−10)	−0.86(−11)
			−0.84(−10)	−0.83(−10)	−0.85(−10)	−0.13(−09)
			−0.84(−10)	−0.84(−10)	−0.85(−10)	−0.13(−09)

3.3. A 3D harmonic oscillator

As an example for solving highly degenerate eigenvalue problems, we consider an isotropic 3D harmonic oscillator with a potential

$$V(x, y, z) = \tfrac{1}{2}(x^2 + y^2 + z^2). \tag{18}$$

Eigenvalues of this case are given by

$$E_{n_x,n_y,n_z} = \tfrac{3}{2} + n_x + n_y + n_z = \tfrac{3}{2} + n, \tag{19}$$

with the degree of degeneracy of $d_n = \frac{(n+1)(n+2)}{2}$ for nth energy level. The present computations use a grid of $22 \times 22 \times 22$ compared to $32 \times 32 \times 32$ used by Braun *et al* [18]. Both results are listed in table 3. Obviously two sets of results reach the same level of accuracy, while the present ones require less than a third of the grid points used by Braun *et al* [18].

Since DSC kernels of Shannon, Dirichlet and MD have very similar behaviour, only the result obtained by the Dirichlet kernel is listed in table 3. The grid points required for the DLVP kernel is still 50% more in each dimension.

3.4. A non-polynomial oscillator

Finally, we consider an NPO model

$$\left[-\frac{\mathrm{d}^2}{\mathrm{d}x^2} + x^2 + \frac{\lambda x^2}{1 + gx^2}\right]\Phi_k = E_k\Phi_k, \tag{20}$$

where λ and g are two parameters. This model has received much attention in the last 20 years for its connection to nonlinear optics, elementary particle physics, and nonlinear Lagrangian field theory. Mitra calculated the ground state and the first excited state using

Table 3. Errors for the eigenvalues of the 3D harmonic oscillator.

n	d_n	Exact	Braun *et al* ($N_x = N_y = N_z = 32$)	Present ($N_x = N_y = N_z = 22$)
0	1	1.5	0.59(−13)	−0.27(−11)
1	3	2.5	0.71(−13)	−0.27(−11)
			0.87(−13)	−0.25(−11)
			0.94(−13)	−0.23(−11)
2	6	3.5	0.20(−12)	−0.27(−11)
			0.23(−12)	−0.20(−11)
			0.36(−11)	−0.19(−11)
			0.36(−11)	0.74(−11)
			0.49(−11)	0.79(−11)
			0.56(−11)	0.79(−11)
3	10	4.5	0.15(−11)	−0.21(−11)
			0.37(−11)	0.57(−11)
			0.37(−11)	0.64(−11)
			0.10(−10)	0.67(−11)
			0.12(−10)	0.72(−11)
			0.27(−10)	0.75(−11)
			0.45(−10)	0.80(−11)
			0.60(−10)	0.83(−10)
			0.68(−10)	0.83(−10)
			0.76(−10)	0.84(−10)

the Ritz variational method in combination with the Givens–Householder matrix eigenvalue algorithm [35]. Finite difference methods are applied to obtain numerical eigenvalues [36, 37]. Kaushal studied asymptotic expansions in terms of gx^2 [38]. Two-parameter scaling transform was employed by Bessis and Bessis [39]. Lai and Lin applied the Hellmann–Feynman and hypervirial theory [40] to calculate eigenvalues from a perturbation series. Flessas showed that exact solutions exist for some special parameters [41]. Varshni [42] and Witwit [43] extended this 1D model to three dimensions. Scherrer *et al* obtained very accurate ground states by using a matrix-continued-fraction algorithm [44] and compared their results with those of other authors.

In general, this model does not have an exact solution. High-accuracy numerical solution to this problem is nontrivial. This can be noted from the potential plot in figure 1. The ground state is extremely sensitive to the bottom shape of the potential. In particular, convergent eigenvalues of large λ and g parameters are difficult to attain. In the present work we employ the DSC algorithm to calculate various ground states associated with a variety of parameters (λ, $g = 1$, 10, 100, and 500). The DSC results are attained by using the MD kernel on a uniform grid. Other kernels perform similarly. Table 4 provides a comparison of the DSC results and results reported in the literature. There are a number of discrepancies among the results of different authors. Our results are in excellent agreement with those of Scherrer *et al* [44]. The DSC results converge to at least 11 significant figures for all parameters calculated. A potential adapted DSC algorithm is under consideration to achieve better convergence.

4. Conclusion

This paper explores the utility of a DSC algorithm for solving the Schrödinger equation. DSC kernels of Shannon, Dirichlet, MD and DLVP are employed for this application. Four

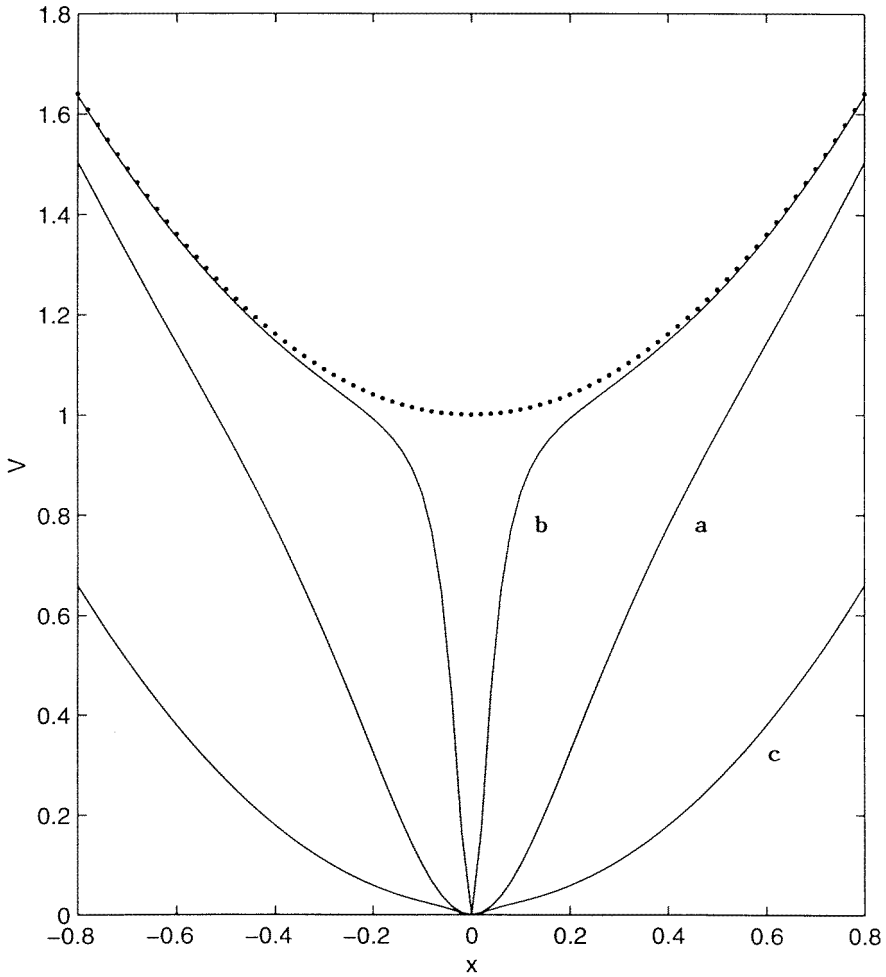

Figure 1. The NPO potential. Values of parameters λ and g are: (*a*) 10, 10; (*b*) 500, 500; (*c*) 10, 500. The dotted curve is the harmonic potential $V(x) = x^2 + \lambda/g$.

benchmark problems are utilized to illustrate the robustness and accuracy of the present approach.

In the first example, a Morse oscillator for the I_2 molecule is examined. The corresponding Schrödinger equation is analytically solvable. The DSC algorithm performs extremely well for this model. The first 25 eigenvalues are accurate to 12 significant figures obtained by using 64 grid points, which is 200 to 1000 times better than those of an efficient Chebyshev–Lanczos method [18], obtained by using 128 grid points. These results are the best to date as far as the author is aware (as produced by using a local approach). The DLVP kernel requires 1.5 times grid points (96 points) to achieve the same level of accuracy as that of other DSC kernels. This result, however, is still about 100 to 1000 times more accurate than those of Braun *et al* [18] obtained using 128 grid points.

The next example is a 2D harmonic oscillator potential. This example is very valuable because it is also analytically solvable. The performances of DSC kernels of Shannon, Dirichlet and MD are excellent: only 26 grid points in each dimension are required to achieve the

Table 4. Ground state eigenvalues of the NPO: (a) Scherrer *et al* [44], (b) Hautot [46], (c) Mitra [35], (d) Bessis *et al* [39], (e) Chaudhuri and Mukherjee [45], (f) Lai and Lin [40], (g) Kaushal [38], (h) Galacia and Killingbeck [36].

		λ			
g		1	10	100	500
1	DSC	1.232 350 723 32	2.782 330 515 89	9.359 418 026 28	21.658 747 700 0
1	(a)	1.232 350 72	2.782 330 52	9.359 418 03	
1	(b)	1.232 35	2.782 33	9.354 2	
1	(c)	1.232 35	2.782 33	9.354	
1	(d)	1.232 372 05	2.782 330	9.359 418 03	21.658 747 7
1	(e)	1.241 3			
1	(f)	1.232 353 53	2.782 330 54	9.359 418 03	
1	(g)	1.227	2.754	9.356 7	
10	DSC	1.059 296 880 81	1.580 022 327 43	5.793 942 300 20	16.732 747 382 0
10	(a)	1.059 296 88	1.580 022 33	5.793 942 30	
10	(b)	1.059 30	1.580 02	5.793 94	
10	(c)	1.059 29	1.580 02	5.794	
10	(d)	1.059 297 00	1.580 024 9	5.793 947	16.739 19
100	DSC	1.008 410 597 89	1.084 063 335 55	1.836 335 833 44	5.083 683 913 46
100	(a)	1.008 410 60	1.084 063 34	1.836 335 83	
100	(b)	1.008 41	1.084 06	1.836 34	
100	(c)	1.008 41	1.084 06	1.836 4	
100	(d)	1.008 410 6	1.084 064 3	1.836 385 0	5.084 085 7
100	(e)		1.084 11	1.841 1	
100	(h)			1.836 337 3	
500	DSC	1.001 849 1547	1.018 491 045 11	1.184 860 239 7	1.923 176 255 4
500	(d)	1.001 8491	1.018 491 0	1.184 863 2	1.923 226 0
500	(e)			1.184 51	1.922 55

accuracy of 11 significant figures for the first 21 eigenvalues. The same level of accuracy is attained by the DLVP kernel using 39 grid points in each dimension.

The third example considered is a 3D harmonic oscillator potential. This is a problem for objectively testing the ability of handling highly degenerate eigenvalues. As in the first example, the present algorithm performs much better than the efficient Chebyshev–Lanczos method [18]. We choose only a grid of $22 \times 22 \times 22$ to achieve the same accuracy as those of Braun *et al* obtained by using a grid of $32 \times 32 \times 32$ (the ratio of the two grid points is $1 : 3.08$).

The last example considered is an NPO. In general, this problem does not have an analytical solution. For a certain parameter region, the low-lying eigenvalues are very sensitive to the sharp variation of the bottom curve in the potential and difficult to converge. There are a lot of discrepancies among the results of different authors in the literature. The present calculation helps to clarify the matter. In particular, our results are in excellent agreement with results of Scherrer *et al* obtained by using a matrix-continued-fraction algorithm [44]. We calculate a number of ground states with at least 11 significant figures. These studies indicate that the DSC algorithm is efficient and reliable for numerically solving the Schrödinger equation.

Acknowledgments

This work was supported in part by the National University of Singapore. The author is grateful to the referees for valuable comments and suggestions.

References

[1] Lanczos C 1938 *J. Math. Phys.* **17** 123
[2] Harris D O, Engerholm G G and Gwinn W D 1965 *J. Chem. Phys.* **43** 1515
[3] Cooley J W and Tukey J W 1965 *Math. Comput.* **19** 297
[4] Finlayson B A and Scriven L E 1966 *Appl. Mech. Rev.* **19** 735
[5] Orszag S A 1972 *Stud. Appl. Math.* **51** 253
[6] Kreiss H O and Oliger J 1972 *Tellus* **24** 199
[7] Finlayson B A 1972 *The Method of Weighted Residuals and Variational Principles* (New York: Academic)
[8] Fornberg B 1973 *Math. Comput.* **27** 45
[9] Lill J V, Parker G A and Light J C 1982 *Chem. Phys. Lett.* **89** 483
[10] Kosloff D and Baysal E 1982 *Geophysics* **47** 1402
[11] Hutson J M and Le Roy R J 1985 *J. Phys. B: At. Mol. Phys.* **83** 1197
[12] Friesner R 1985 *Chem. Phys. Lett.* **116** 39
[13] Yang W and Peet A C 1988 *Chem. Phys. Lett.* **153** 98
[14] Schwenke D W and Truhlar D G 1990 *Computing Methods in Applied Sciences and Engineering* ed R Glowinski and A Lichnewsky (Philadelphia, PA: SIAM)
[15] Hoffman D K, Nayar N, Sharafeddin O A and Kouri D J 1991 *J. Phys. Chem.* **95** 8299
[16] Colbert D T and Miller W H 1992 *J. Phys. Chem.* **96** 1982
[17] Fornberg B 1996 *A Practical Guide to Pseudospectral Methods* (Cambridge: Cambridge University Press)
[18] Braun M, Sofianos S A, Papageorgiou D G and Lagaris I E 1996 *J. Comput. Phys.* **126** 315
[19] Wei G W 1998 *Chem. Phys. Lett.* **296** 215
[20] Hu X G, Ho T S and Rabitz H 1998 *Comput. Phys. Commun.* **113** 168
[21] Wei G W 1999 *J. Chem. Phys.* **110** 8930
[22] Wei G W *Physica* D at press
[23] Wei G W 1999 *Advanced Signal Processing Algorithms, Architectures, and Implementations* vol 9, ed F T Luk (Bellingham: SPIE Optical Engineering Press) pp 112–22
Wei G W *J. Chem. Phys.* submitted
[24] Schwartz L 1951 *Théore des Distributions* (Paris: Hermann)
[25] Korevaar J 1955 *Ned. Akad. Westensh. Proc. Ser.* A **58** 368
Korevaar J 1968 *Mathematical Methods* vol 1 (New York: Academic)
[26] Korevaar J 1959 *Trans. Am. Math. Soc.* **91** 53
[27] Walter G G 1965 *Trans. Am. Math. Soc.* **116** 492
[28] Walson G W and Leadbetter M R 1965 *Sankhya* **26** 101
[29] Winter B B 1975 *Ann. Statist.* **3** 759
[30] Walter G G and Blum J 1977 *Ann. Statist.* **7** 328
[31] Walter G G 1992 *Wavelets, A Tutorial in Theory and Applications* ed C K Chui (San Diego, CA: Academic)
[32] Wahba G 1975 *Ann. Statist.* **3** 15
[33] Kronmal R and Tarter M 1968 *J. Am. Statist. Assoc.* **63** 925
[34] Flügge S 1974 *Practical Quantum Mechanics* (New York: Springer)
[35] Mitra A K 1978 *J. Math. Phys.* **19** 2018
[36] Galicia S and Killingbeck J P 1979 *Phys. Lett.* A **71** 17
[37] Fack V and Vanden Berghe G 1985 *J. Phys. A: Math. Gen.* **27** 3355
[38] Kaushal R S 1979 *J. Phys. A: Math. Gen.* **12** L253
[39] Bessis N and Bessis G 1980 *J. Math. Phys.* **21** 2780
[40] Lai C L and Lin H E 1982 *J. Phys. A: Math. Gen.* **15** 1495
[41] Flessas G P 1981 *Phys. Lett.* A **83** 121
[42] Varshni Y P 1987 *Phys. Rev.* A **36** 3009
[43] Witwit M R M 1996 *J. Comput. Phys.* **129** 220
[44] Scherrer H, Risken H and Leiber T 1988 *Phys. Rev.* A **38** 3949
[45] Chaudhuri R N and Mukherjee B 1983 *J. Phys. A: Math. Gen.* **16** 4031
[46] Hautot A 1981 *J. Comput. Phys.* **39** 72